ChemPubSoc Europe

DOI: 10.1002/cctc.201600650

CHEMCATCHEM Full Papers

Suppression of the Aromatic Cycle in Methanol-to-Olefins Reaction over ZSM-5 by Post-Synthetic Modification Using Calcium

Irina Yarulina,[a] Simon Bailleul,[b] Alexey Pustovarenko,[a] Javier Ruiz Martinez,[c] Kristof De Wispelaere,[b] Julianna Hajek,[b] Bert M. Weckhuysen,[c] Klaartje Houben,[d] Marc Baldus,[d] Veronique Van Speybroeck,[b] Freek Kapteijn,[a] and Jorge Gascon*[a]

Incorporation of Ca in ZSM-5 results in a twofold increase of propylene selectivity (53%), a total light-olefin selectivity of 90%, and a nine times longer catalyst lifetime (throughput 792 $g_{MeOH}\,g_{catalyst}^{-1}$) in the methanol-to-olefins (MTO) reaction. Analysis of the product distribution and theoretical calculations reveal that post-synthetic modification with Ca^{2+} leads to the formation of $CaOCaOH^{+}$ that strongly weaken the acid strength of the zeolite. As a result, the rate of hydride transfer and oligomerization reactions on these sites is greatly reduced, resulting in the suppression of the aromatic cycle. Our results further highlight the importance of acid strength on product selectivity and zeolite lifetime in MTO chemistry.

Introduction

The discovery of the methanol-to-gasoline (MTG) process over ZSM-5 catalysts by Mobil Corporation in 1977[1] opened an oil-free route for the synthesis of hydrocarbons. Since then, a great deal of effort has been devoted to mechanistic studies that led to a better understanding of this catalytic process.

The evolution in mechanism comprehension started from understanding the first C–C bond formation (which is still under the debate)[2] and slowly developed to the currently accepted dual-cycle concept.[3] An important milestone in methanol-to-olefins (MTO) history was the introduction of the "hydrocarbon pool" concept by Dahl and Kolboe, who proposed the existence of intermediates of coke deposits responsible for olefin formation.[4] These intermediates were later clarified to be methylbenzenes and/or their protonated versions.[5] Transient $^{12}C/^{13}C$ experiments, however, revealed that whereas ethylene is predominantly formed through the abovementioned aromatic species, propylene and higher alkenes are formed from olefin methylation and cracking reactions.[3b,5] These observations led to the acceptance of the dual-cycle mechanism, involving the presence of two cycles, namely, a methylation/cracking cycle, in which mostly propylene is produced, and an aromatic cycle, responsible for ethylene and aromatics formation and catalyst deactivation.

Sun et al. have shown that one cycle can be promoted over the other by co-feeding species participating in these cycles, that is, co-feeding of propylene led to the increased selectivity of olefinic species, whereas co-feeding of aromatics promoted the formation of methane, ethylene and aromatic species.[3c,6]

An approach to suppress the aromatic cycle is currently of utmost interest as it is the key to prolong catalyst lifetime and to increase the selectivity to propylene. Teketel et al. have shown, using ZSM-22, that by choosing the appropriate zeolite topology the methylation/cracking cycle can be promoted over the aromatic one.[7,8]

Considering that aromatic species are formed from higher alkenes, another approach to suppress the aromatic cycle would involve tuning the acidity of the catalyst, since less acidic catalysts are known to promote the alkene cycle.[9] In this way, it would be possible to produce olefins via the methylation/cracking cycle but their further conversion to aromatics would be restricted.

Some studies, mainly performed in the early 1990s, showed that modification of ZSM-5 with elements such as Ca,[10] B[11] or

[a] I. Yarulina, A. Pustovarenko, Prof. Dr. F. Kapteijn, Prof. Dr. J. Gascon
Catalysis Engineering Group, Department of Chemical Engineering, Faculty of Applied Sciences
Delft University of Technology
Julianalaan 136
2628 BL Delft (The Netherlands)
E-mail: j.gascon@tudelft.nl

[b] S. Bailleul, Dr. K. D. Wispelaere, J. Hajek, Prof. Dr. V. V. Speybroeck
Center for Molecular Modeling
Ghent University
Technologiepark 903
9052 Zwijnaarde (Belgium)

[c] Dr. J. R. Martinez, Prof. Dr. B. M. Weckhuysen
Inorganic Chemistry and Catalysis Group, Debye Institute for Nanomaterials Science
Utrecht University
Universiteitsweg 99
3584 CG Utrecht (The Netherlands)

[d] Dr. K. Houben, Prof. Dr. M. Baldus
NMR Research Group, Debye Institute for Nanomaterials Science
Utrecht University
Universiteitsweg 99
3584 CG Utrecht (The Netherlands)

Supporting information and the ORCID identification number(s) for the author(s) of this article can be found under http://dx.doi.org/10.1002/cctc.201600650.

P[12] leads to the increased formation of olefins. Many of these results were very promising but did not receive the worthwhile attention as "the most valuable ethylene was formed very little".[13] Nowadays, the industrial focus has shifted towards propylene. The observed high selectivities to propylene and butenes and low selectivities to ethylene are already indicative that this modification might result in the promotion of the olefinic cycle over the aromatic cycle.

Results and Discussion

In this work, we modified the ZSM-5 acidity by Ca incorporation and investigated, using a combined experimental and theoretical approach, how this modification changes the nature of the acid sites, which in turn leads to the suppression of the aromatic cycle in favour of the olefinic cycle, leading to enhanced propylene formation.

The parent ZSM-5 zeolite used for the preparation of the Ca containing catalysts was purchased from Zeolyst (Si/Al = 40, CBV8014). Depending on the method of preparation, the obtained catalysts are denoted as Ca-ZSM5-IE, 6 Ca-ZSM-5-SSIE, 6 Ca-ZSM5-IWI, 6 Ca-ZSM5-EW, where IE, SSIE, IWI and EW stand for ion-exchange, solid state ion-exchange, incipient wetness impregnation and wet impregnation, respectively. All catalysts were prepared aiming at a 6 wt. % Ca loading. Another set of catalysts was prepared by incipient wetness impregnation by varying Ca loading from 1 to 6 wt. % respectively. Details about catalyst preparation can be found in the Experimental Section. XRD results show (Figure S1, Supporting Information) that the original MFI topology is preserved in all samples.[12a]

Textural properties displayed in Table 1 demonstrate that Ca incorporation produces a small decrease in micropore volume, whereas no additional mesopores are created. NH_3 temperature-programmed desorption (TPD) results (Table 1 and Figure 1 a) show that the concentration of acid sites for all catalysts except 6 Ca-ZSM5-SSIE is similar to that of the parent ZSM-5, whereas the desorption maximum shifts from 435 °C to 290 °C for 6 Ca-ZSM5-EW and 6Ca-ZSM5-IWI, already indicating a qualitative weakening in the strength of these acid sites upon Ca incorporation. As NH_3 TPD is not an adequate tool to quantify the nature and strength of acid sites,[14] the catalysts under study were additionally characterized by FTIR spectroscopy using pyridine as a probe molecule (Figure 1 b). Parent ZSM-5 shows two IR bands at 1546 cm^{-1} and 1455 cm^{-1} representing adsorption of pyridine on Brønsted and Lewis acid sites, respectively. The Lewis acidity in the parent zeolite is ascribed to extra-framework Al species[15] but can be the result of both extra-framework and perturbed framework Al.[16] Incorporation of Ca into the zeolite caused a significant decrease of Brønsted acidity for all samples, especially for 6 Ca-ZSM5-EW and 6 Ca-ZSM5-IWI, for which the vibration at 1545 cm^{-1} almost completely disappeared. Direct observation of the zeolite IR spectrum in Figure 1 c shows a similar disappearance of the 3600 cm^{-1} band characteristic for the Brønsted hydroxyl stretching. Along with the disappearance of Brønsted acidity, a new pyridine band at 1446 cm^{-1}, assigned to acid sites of Lewis nature, arises for Ca-containing catalysts, indicating transformation of strong Brønsted acid sites to Lewis acid ones. Interestingly, Ca-ZSM5-IE displays both IR bands at 1455 and 1446 cm^{-1} and can be considered as in between ZSM-5 and 6 Ca-ZSM5-IWI, having intermediate acidic properties. FTIR spectroscopy using CO as a probe molecule (Figure S2) further confirms the transformation of Brønsted into Lewis acid sites and suggests the existence of Ca sites of different nature.

To obtain a full picture of the acidic properties of these catalysts, we performed additional characterization by solid-state NMR spectrometry using trimethylphosphine oxide (TMPO) as a probe molecule (Figure 1 d). Several ^{31}P resonance peaks at 99, 75, 67, 63, 47, 43, 36 and 30 ppm are observed. The resonance peak at 30 ppm is ascribed to "mobile" TMPO, and peaks at 47, 43 and 36 ppm are characteristic for physisorbed TMPO.[17] Peaks in the range between 60 and 90 ppm are arising from $TMPOH^+$ complexes on Brønsted acid sites.[18] The peak at 99 ppm can be attributed to very strong Lewis acid sites.[19] Adsorption of TMPO on Ca-ZSM5-IE resulted in the appearance of similar peaks, however, a significant decrease of the resonance at 67 ppm suggests that, during ion exchange, Ca preferentially occupies certain Brønsted acid sites. In contrast, in the spectra of 6 Ca-ZSM5-IWI the peaks in the 60–90 ppm range are absent. In summary, the extensive acidity characterization performed demonstrates the transformation of Brønsted into Lewis acidity.

The as-prepared catalysts were tested at 500 °C in the MTO reaction. Such a relatively high reaction temperature was

Table 1. Textural and catalytic properties of the ZSM-5 catalyst materials under study.

Entry	Catalyst	V_{total}[a] [$cm^3\,g^{-1}$]	V_{micro}[a] [$cm^3\,g^{-1}$]	S_{BET}[a] [$m^2\,g^{-1}$]	S_{micro}[a] [$m^2\,g^{-1}$]	c_{AS}[b] [$\mu mol\,g^{-1}$]	c_{BAS}[c] [$\mu mol\,g^{-1}$]	c_{LAS}[c] [$\mu mol\,g^{-1}$]	Throughput[d] [$g_{MeOH}\,g_{catalyst}^{-1}$]	$S(C_{3=})$ [C mol %]
1	ZSM-5	0.256	0.152	448	363	387	232	35	88	25
2	Ca-ZSM5-IE	0.273	0.145	429	344	402	138	108	264	39
3	6 Ca-ZSM5-SSIE	0.212	0.111	323	267	171	128	0	136	39
4	6 Ca-ZSM5-EW	0.199	0.110	336	276	374	38	208	304	43
5	6 Ca-ZSM5-IWI	0.226	0.124	385	310	384	29	240	504	53
6	4 Ca-ZSM5-IWI	0.223	0.126	387	313	381	27	240	480	45
7	2 Ca-ZSM5-IWI	0.238	0.128	392	315	332	40	228	792	39
8	1 Ca-ZSM5-IWI	0.246	0.138	418	334	347	66	198	272	46

[a] From N_2 adsorption. [b] Concentration of acid sites (AS) derived from NH_3 TPD. [c] Concentration of Brønsted (BAS) and Lewis (LAS) acid sites derived from pyridine IR spectroscopy. [d] Amount of methanol (g) converted per gram of zeolite before conversion decreases below 80 %.

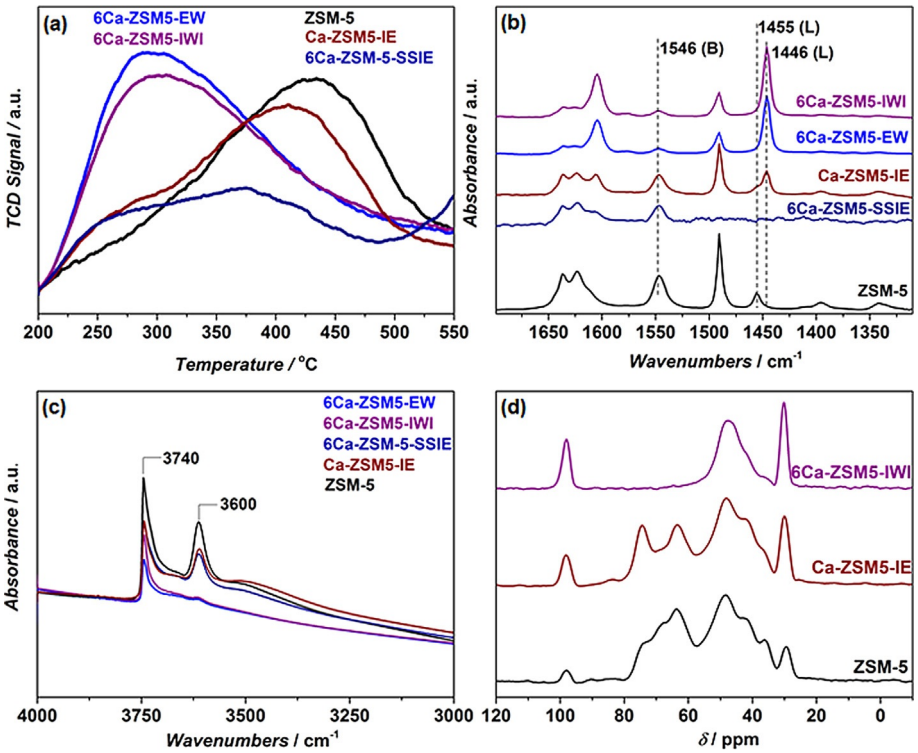

Figure 1. Acidity characterization of Ca-containing ZSM-5 catalysts and parent ZSM-5. (a) NH_3 TPD profiles, (b) FTIR spectra of adsorbed pyridine, (c) FTIR spectra in the OH stretching region, (d) ^{1}H-^{31}P CP MAS NMR spectra for TMPO adsorbed on 6 Ca-ZSM5-IWI, Ca-ZSM5-IE and ZSM-5.

chosen because higher temperatures favour the formation of short chain olefins.[20] Furthermore, owing to their lower acidity, some of the catalysts were not catalytically active below 475 °C. The conversion results in Figure 2 a demonstrate that incorporation of Ca into ZSM-5 prolong catalyst lifetime. Herein, the method of catalyst preparation is crucial to obtain the longest lifetime and selectivity to propylene, and the best results were obtained by using the catalyst prepared by IWI (504 vs. 88 g MeOH converted per gram of catalyst). As shown above, other preparation methods are less effective in weakening zeolite acidity and led to shorter catalyst lifetimes. Remarkably, Ca incorporation caused significant changes in product distribution (Figure 2 b), the most important of which are the decrease in the formation of paraffins and ethylene. For 6 Ca-ZSM5-IWI and 6 Ca-ZSM5-EW, the selectivity to paraffins drops from 27 down to 3 %, and the selectivity to ethylene from 16 % down to 8 and 6 %, respectively, compared with the performance of parent ZSM-5. Moreover, 6 Ca-ZSM5-IWI showed only negligible formation of aromatics in comparison to parent ZSM-5 (compare S_{C6-8} = 0.5 % and 9 % respectively, Figure 2). Both, the much lower selectivity to aromatics along with smaller ethylene productivity indicate—to a large extent—the suppression of the aromatic cycle. Indeed, ethylene is considered to be the main product of this cycle.[3b,5,21] On the other hand, the lower paraffin selectivity indicates the partial suppression of intermolecular hydride transfer reactions responsible for the conversion of olefins to paraffins and aromatics.[21a] The latter is considered to be the bridging step between the olefinic and aromatic cycles. We thus conclude that the observed suppres-

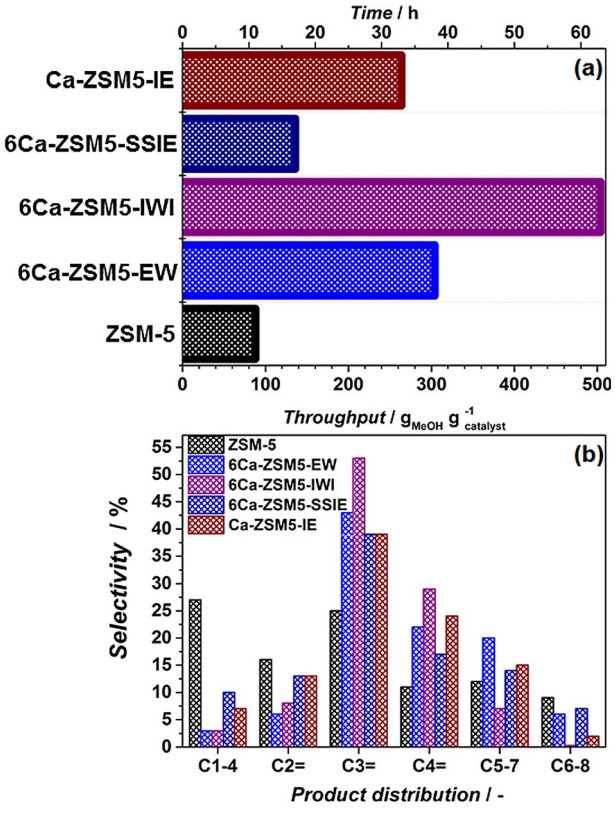

Figure 2. Methanol conversion over Ca-modified ZSM-5 prepared by different methods tested at 500 °C in MTO. (a) Catalyst lifetime, (b) product distribution. m_{cat} = 0.5 g, WHSV = 8 $g_{MeOH}\,g_{catalyst}^{-1}\,h^{-1}$, MeOH/$N_2$ = 1:1.

sion of the aromatic cycle is achieved by reducing the rate of hydride transfer and oligomerisation reactions on significantly weaker acid sites.[22]

As catalyst 6Ca-ZSM5-IWI prepared by IWI showed the highest selectivity to propylene (53%) and butenes (29%) and the longest lifetime, this method was used to further to optimize the Ca content. NH_3 TPD and pyridine FTIR spectrometry (Figures S3 and S4) reveal that all samples possess a similar concentration of acid sites and modification with Ca caused almost complete disappearance of Brønsted acidity as was observed for 6Ca-ZSM5-IWI.

Catalytic experiments (Figure 3) showed that by employing a Ca loading of 2 wt.% with a molar ratio of Ca to Al 2:1

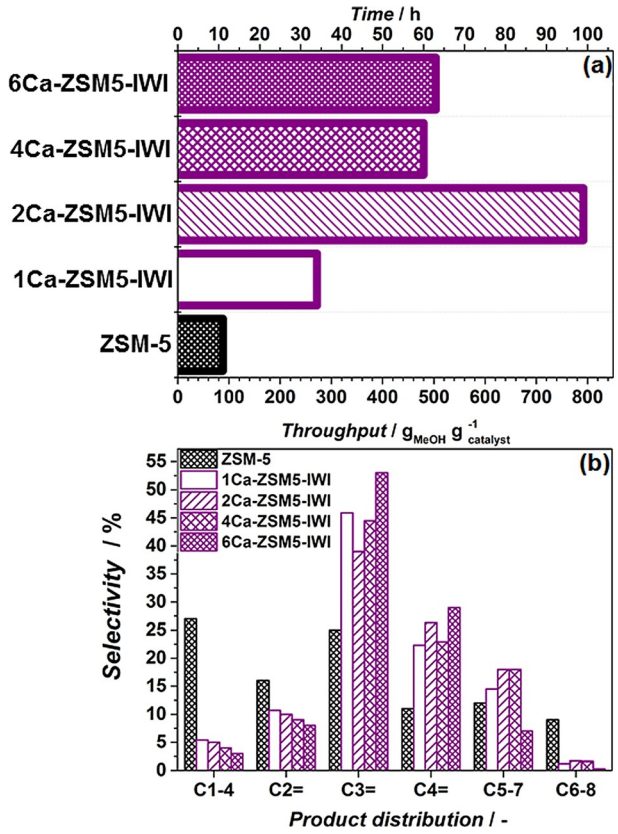

Figure 3. Methanol conversion over Ca-modified ZSM-5 prepared by the IWI method with different Ca loading tested at 500 °C in MTO. (a) Catalyst lifetime, (b) product distribution. $m_{cat} = 0.5$ g, WHSV = 8 $g_{MeOH}\, g_{catalyst}^{-1}\, h^{-1}$, $MeOH/N_2 = 1{:}1$.

(Table S1), catalyst lifetime was further prolonged up to 99 h, corresponding to 792 g of MeOH converted per gram of catalyst before the catalyst became fully deactivated, which is nine times longer than for the commercial ZSM-5. The selectivities to propylene (39%) and butenes (26%) were slightly lower than for 6Ca-ZSM5-IWI. Observed differences in selectivities caused by different Ca loadings are tentatively attributed to additional spatial restrictions caused by Ca deposition inside the micropores, that is, reducing micropore volume (see Table 1), resulting in less aromatics formation, thus enhancing formation of propylene and decreasing formation of ethylene (Figure 3b). However, based on toluene adsorption isotherms (Figure S5), shape selective effects can be ruled out. Whether bulkier aromatic molecules,[12b,21a] as suggested by Abubakar et al.[23] on P-modified ZSM-5, can be formed inside of the pores of the Ca modified ZSM-5 catalyst is still not clear.

As mentioned in the introduction, a great deal of effort has been dedicated in the open literature to the modification of acid sites and its consequences in MTO performance,[24] including Ca modification.[10a,b,25] For example, Zhang et al. modified ZSM-5 with $Ca(NO_3)_2$ to achieve a propylene selectivity up to 50% with catalyst lifetime increasing from 13 to 75 h at WHSV = 4.2 h^{-1}.[10b] Observed differences were attributed to the acid site weakening through the formation of acid-base centres but without spectroscopic evidence to support this hypothesis. Nonetheless, the observed large decrease in paraffin and ethylene selectivities was not discussed either by these authors. High selectivity towards propylene is generally demonstrated for mesoporous ZSM-5.[26] It is claimed that this is a result of both improved diffusion properties and acid site strength modification. However, according to Olsbye et al.[27] the observed differences are not yet satisfactorily described and explained. By creating mesopores in ZSM-5, Mei et al. reached a selectivity to propylene of approximately 42% together with a considerable drop in the production of paraffins (from 20.5 down to 5.7%) and ethylene (from 15.3 down to 4.2%).[26a] These results were rationalized on the basis of a different contribution of the aromatic and olefinic route, that is, by partial suppression of the aromatic cycle.

On the other hand, the modification of the acidity might simply lead to a decreased amount of working acid sites, i.e. partial poisoning. Thus, application of ZSM-5 with a high SiO_2/Al_2O_3 ratio, and therefore a much lower density of acid sites, has been widely reported with light olefin selectivity increasing upon decreasing Al content.[28] Although very effective in terms of selectivity, these zeolites with low Al content usually deactivate faster[12a] owing to selective coke deposition on the few active sites. We tentatively suggest that the promotional effect of acid site modification is mainly related to the decreasing the strength of acid sites rather than their amount. Thus, the biggest difference between decreasing Al content and "poisoning" (or "modifying") acid sites with Ca is that in the former case the amount of acid sites has been lowered whereas in the latter their strength has been weakened through changing their nature but preserving their amount.

To obtain molecular level insight into the nature of the active site of the pristine and Ca-modified catalysts, a set of periodic DFT calculations were performed using the Vienna Ab Initio Simulation Package (VASP).[29] Simulation details are provided in the Supporting Information.[30] Inspired by earlier literature reports[10a,31] and the experimentally defined optimal Ca:Al ratio of 2, we calculated the electronic energies for a systematic set of $CaOCaOH^+$ structures coordinated to framework oxygen atoms near the Al substitution and with different orientations in the channel intersections (Figures S10 and S11). An overview of all considered structures is given in the Supporting Information. We assumed isolated Brønsted acid sites in the pristine H-ZSM-5 material, which is a realistic representa-

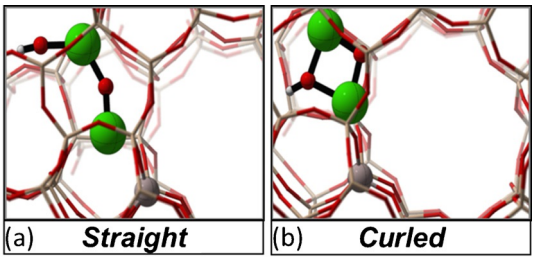

Figure 4. Representation of suggested active sites in Ca-ZSM-5 with (a) straight and (b) curled configuration. Color code: H white, O red, Al grey, Si cream and Ca green.

tion since the experimentally used Si/Al ratio amounts to 40. We observed two stable configurations of Ca species as displayed in Figure 4: the $CaOCaOH^+$ tail may adopt either a straight (Figure 4a) or curled (Figure 4b) configuration. The latter is electronically more stable. A detailed comparison of the vibrational frequencies of the modified Ca-ZSM-5 and pristine ZSM-5 yields some distinct differences for the Ca-modified ZSM-5 catalyst. The calculated OH stretch frequency of the H-ZSM-5 catalyst at 3684 cm^{-1} shifts upwards to 3848 cm^{-1} and 3796 cm^{-1} for the straight and curled Ca chains in the Ca-ZSM-5 catalyst, respectively, located in the range of less acidic silanol groups (3740 cm^{-1}), which corresponds to the spectra shown in Figure 1c.[32] These calculations suggest that the active site in Ca-ZSM-5 catalysts is a combination of multiple $CaOCaOH^+$ structures, and the shift of the OH stretch frequencies points towards a lower Brønsted acidity of the calcium-modified catalyst.

Conclusions

The post-synthetic incorporation of Ca into ZSM-5 leads to the formation of $CaOCaOH^+$ species that strongly weaken the acid strength of the parent zeolite. As a result, the rates of hydride transfer and oligomerisation reactions on these sites are greatly reduced, resulting in the suppression of the aromatic cycle and to increased total light olefin selectivity in the range of 90%. These results further demonstrate the importance of acid strength on product selectivity and zeolite lifetime in MTO chemistry.

Experimental Section

Synthesis of catalysts

Ca-modified ZSM-5 catalysts were prepared from commercial ZSM-5 (Zeolyst, CBV 8014). Ca-ZSM5-IE was prepared by ion- exchange with 1 M $Ca(NO_3)_2{\cdot}4H_2O$ solution at 80 °C for 2 h repeated three times with filtration step in between and followed by calcination at 550 °C. 6Ca-ZSM5-SSIE was prepared by solid-state ion-exchange with $Ca(CH_3COO)_2$. SSIE was achieved by grinding required amount of calcium acetate with commercial ZSM-5 for 30 min in a mortar followed by calcination at 550 °C. 6Ca-ZSM5-EW was prepared by wet impregnation. In a typical procedure the required amount of $Ca(NO_3)_2{\cdot}4H_2O$ was dissolved in water (5 mL). Zeolite (4 g) was added to this solution and left overnight under stirring at RT. Subsequently, the catalyst was dried for 12 h at 80 °C and calcined at 550 °C. 6Ca-ZSM5-IWI, 4Ca-ZSM5-IWI, 2Ca-ZSM5-IWI and 1Ca-ZSM5-IWI were prepared by incipient wetness impregnation (IWI). Parent zeolite (4 g) was impregnated with $Ca(NO_3)_2{\cdot}4H_2O$ solution (1.06 g) corresponding to the total pore volume of the zeolite. After impregnation, the catalysts were kept overnight in a desiccator followed by drying for 12 h at 80 °C and calcination at 550 °C. A heating rate of 2 °C min^{-1} and static air conditions were applied in all cases for calcination.

Characterization of catalysts

N_2 adsorption at 77 K was performed by using the Tristar II 3020 analyzer (Micromeritics). Prior to the experiment, samples were outgassed at 350 °C for 16 h. Toluene adsorption measurements were performed at 25 °C using Micromeritics 3Flex equipped with a 15 mL stainless steel vapor vessel.

Images were recorded by using a JEOL JSM-6010LA with a standard beam potential of 10 kV and an Everhart–Thornley detector. X-ray microanalysis (SEM/EDX) confirmed the elemental composition in the sample by scanning microscopy (SEM) coupled with a dispersive X-ray microanalysis system (EDX) with a Silicon-drift detector.

The XRD patterns of the powders are recorded in Bragg–Brentano geometry with a Bruker D8 Advance X-ray diffractometer equipped with a LynxEye position-sensitive detector. Measurements were performed at RT by using monochromatic $Co_{K\alpha}$ ($\lambda = 1.788970$ Å) radiation between $2\theta = 5°$ and 50°. Elemental analysis was performed with a PerkinElmer Optima 4300 DV instrument. The samples were first digested in an aqueous mixture of 1% HF and 1.25% H_2SO_4. After dilution, analysis was done by inductively coupled plasma optical emission spectrometry (ICP-OES).

Temperature-programmed NH_3 desorption (NH_3-TPD) was performed with an AutoChem II chemisorption analyzer (Micromeritics). Approximately 0.2 g of the material was first degassed under He flow at 400 °C and then saturated with NH_3 at 200 °C during 1 h using a flow of 1.65% NH_3 in He. The gas mixture was then switched back to He and the sample was purged at 200 °C for about 1 h to remove weakly adsorbed NH_3 molecules. TPD was subsequently recorded under He flow, from 200 °C to 800 °C. All flow rates were adjusted to 25 mL min^{-1}, and the heating rate was 10 °C min^{-1} during the different stages of the experiment.

Transmission FTIR spectroscopy using CO as a probe molecule was performed by using a Nicolet Nexus spectrometer at 4 cm^{-1} resolution equipped with an extended KBr beam splitting and a mercury cadmium telluride (MCT) cryo-detector. The pellets were placed in an IR quartz cell equipped with CaF_2 windows. A movable sample holder allows the sample to be placed in the infrared beam for the measurements or into the furnace for thermal treatments. The cell was connected to a vacuum line for pretreatment. The specimen was activated in vacuum at 400 °C for 16 h to remove adsorbed species. After this step, the samples were cooled down to −130 °C and CO was dosed up to 30 mbar.

Transmission FTIR spectroscopy using pyridine as a probe molecule was performed by using a Nicolet 6700 spectrometer equipped with MCT/B detector. The specimen was activated in vacuum at 400 °C for 16 h to remove adsorbed species. After activation, pellets were saturated with pyridine vapor and further evacuated at 160 °C for 2 h. Spectra were recorded in 1000–4000 cm^{-1} range at 4 cm^{-1} resolution and co-addition of 128 scans. The amount of Brønsted (BAS) and Lewis (LAS) acid sites was derived from the bands at 1545 and 1456 cm^{-1} as described elsewhere using extinc-

tion coefficients of 1.67 and 2.22 respectively.[15,33] Assuming that one molecule of pyridine is adsorbed on one acid site, the following expressions were used to calculate C_{BAS} and C_{LAS}.[33]

$$C_{BAS} = 1.88 \times IA(B) \times R^2/W \quad (1)$$

$$C_{LAS} = 1.42 \times IA(L) \times R^2/W \quad (2)$$

where *IA* (BAS, LAS) is the integrated absorbance of BAS or LAS band (cm^{-1}), *R* is the radius of catalyst disk (cm), and *W* is the mass of catalyst (mg).

For solid-state NMR measurements using trimethoxyphosphine oxide (TMPO) as a probe molecule, the preparation procedure was adapted from Wiper et al.[34] TMPO (50 mg) was dissolved in anhydrous CH_2Cl_2 (15 mL) in an Ar glove box. A 15 mL volume of this solution was added to the dehydrated at 400 °C for 16 h zeolite and left under stirring for 1 h. Subsequently, materials were heated at 150 °C for 1 h under vacuum to allow homogeneous distribution of TMPO. Finally, cooled down samples were transferred into a zirconia MAS rotor (3.2 mm). Solid-state ^{31}P NMR spectra were recorded on a Bruker spectrometer operating at a ^{1}H Larmor frequency of 500 MHz equipped with a triple resonance 3.2 mm Magic Angle Spinning (MAS) probe, using an MAS frequency of 19 kHz. After a ^{1}H 90 pulse, ^{1}H-^{31}P cross-polarization (CP) was achieved by applying simultaneously a 46 kHz ^{31}P and a 94 kHz ^{1}H RF field (ramp 70–100%) with a contact time of 4.2 ms. During acquisition 83 kHz SPINAL64 proton decoupling[35] was applied. For each experiment, 256 scans were used with a recycle delay of 4 s.

Methanol-to-olefins testing

Catalytic experiments were performed in a Microactivity Reference unit (PID Eng&Tech) at 500 °C and ambient pressure. The catalyst (pressed, crushed and sieved to particle sizes 250–420 μm) was placed in a fixed-bed reactor with internal diameter 9 mm for standard experiments. An HPLC pump (307 5-SC-type piston pump, Gilson) was used to feed methanol to the reactor system. A weight-hourly space velocity (WHSV) of 8 $g_{MeOH}\,g_{cat}^{-1}\,h^{-1}$, a 1:1 molar feed composition of N_2 and MeOH and atmospheric pressure were utilized. The product mixture was analyzed online with an Interscience CompactGC equipped with a 15 m capillary RTX-1 (1% diphenyl-, 99% dimethylpolysiloxane) column and a flame ionization detector. Conversion, selectivities and yields were calculated on a molar carbon basis. Thus, conversion was defined as the carbon based fraction of light oxygenates (methanol and dimethyl ether) consumed during the reaction:

$$X = \frac{n_{C,MeOH_{in}} - n_{C,MeOH_{out}} - 2 \times n_{C,DME_{out}}}{n_{C,MeOH_{in}}} \times 100\% \quad (3)$$

The selectivity towards ethylene (2) and propylene (3) was calculated based on the carbon number as follows:

$$S_{ethylene} = \frac{2 \times n_{C_2H_4}}{n_{C,MeOH_{in}} - n_{C,oxy_{out}}} \times 100\% \quad (4)$$

$$S_{propylene} = \frac{3 \times n_{C_3H_6}}{n_{C,MeOH_{in}} - n_{C,oxy_{out}}} \times 100\% \quad (5)$$

and the yield of a component *i* was defined from its selectivity and methanol conversion:

$$Y_i = \frac{S_i \times X}{100} \quad (6)$$

The performance results were presented in graphs as a function of the methanol throughput per amount of catalyst used ($g_{MeOH}\,g_{cat}^{-1}$) and defined as overall MeOH throughput fed through the catalytic bed before the conversion of oxygenates drops to 80%. Selectivities were taken after testing catalysts for 1.5 h. Remarkably, for Ca-modified samples the steady state was achieved after approximately 40 min on stream and product distribution did not change significantly (Figure S6) after that time. For ZSM-5, no steady state was achieved, and the early stages were characterized by the high selectivity towards paraffins decreasing with time on stream in favor of olefins.

Acknowledgements

This research received funding from the Netherlands Organisation for Scientific Research (NWO) in the framework of the TASC Technology Area "Syngas, a Switch to Flexible New Feedstock for the Chemical Industry (TA-Syngas)". K.D.W., S.B., J.H. and V.V.S. acknowledge the Foundation of Scientific Research, Flanders (FWO), the Research Board of Ghent University, and the European Union's Horizon 2020 research and innovation programme (consolidator ERC grant agreement No. 647755—DYNPOR (2015–2020)). Computational resources and services were provided by the Stevin Supercomputer Infrastructure of Ghent University and by the Flemish Supercomputer Center (VSC), funded by the Hercules Foundation and the Flemish Government—department EWI.

Keywords: acidity · alkenes · calcium · density functional calculations · zeolites

[1] C. D. Chang, C. T. W. Chu, Mobil Oil Corp, **1977**.
[2] a) A. Comas-Vives, M. Valla, C. Copéret, P. Sautet, *ACS Cent. Sci.* **2015**, *1*, 313–319; b) D. Lesthaeghe, V. Van Speybroeck, G. B. Marin, M. Waroquier, *Angew. Chem. Int. Ed.* **2006**, *45*, 1714–1719; *Angew. Chem.* **2006**, *118*, 1746–1751.
[3] a) K. Hemelsoet, J. Van der Mynsbrugge, K. De Wispelaere, M. Waroquier, V. Van Speybroeck, *ChemPhysChem* **2013**, *14*, 1526–1545; b) U. Olsbye, S. Svelle, M. Bjorgen, P. Beato, T. V. W. Janssens, F. Joensen, S. Bordiga, K. P. Lillerud, *Angew. Chem. Int. Ed.* **2012**, *51*, 5810–5831; *Angew. Chem.* **2012**, *124*, 5910–5933; c) X. Sun, S. Mueller, Y. Liu, H. Shi, G. L. Haller, M. Sanchez-Sanchez, A. C. van Veen, J. A. Lercher, *J. Catal.* **2014**, *317*, 185–197.
[4] I. M. Dahl, S. Kolboe, *Catal. Lett.* **1993**, *20*, 329–336.
[5] M. Bjorgen, S. Svelle, F. Joensen, J. Nerlov, S. Kolboe, F. Bonino, L. Palumbo, S. Bordiga, U. Olsbye, *J. Catal.* **2007**, *249*, 195–207.
[6] X. Sun, S. Mueller, H. Shi, G. L. Haller, M. Sanchez-Sanchez, A. C. van Veen, J. A. Lercher, *J. Catal.* **2014**, *314*, 21–31.
[7] S. Teketel, W. Skistad, S. Benard, U. Olsbye, K. P. Lillerud, P. Beato, S. Svelle, *ACS Catal.* **2012**, *2*, 26–37.
[8] S. Teketel, L. F. Lundegaard, W. Skistad, S. M. Chavan, U. Olsbye, K. P. Lillerud, P. Beato, S. Svelle, *J. Catal.* **2015**, *327*, 22–32.
[9] M. W. Erichsen, K. De Wispelaere, K. Hemelsoet, S. L. C. Moors, T. Deconinck, M. Waroquier, S. Svelle, V. Van Speybroeck, U. Olsbye, *J. Catal.* **2015**, *328*, 186–196.
[10] a) S. Zhang, B. Zhang, Z. Gao, Y. Han, *Ind. Eng. Chem. Res.* **2010**, *49*, 2103–2106; b) S. Zhang, B. Zhang, Z. Gao, Y. Han, *React. Kinet. Mech. Catal.* **2010**, *99*, 447–453; c) A. M. Al-Jarallah, U. A. El-Nafaty, M. M. Abdillahi, *Appl. Catal. A* **1997**, *154*, 117–127.

[11] N. V. Klyueva, N. D. Tien, K. G. Ione, *React. Kinet. Catal. Lett.* **1985**, *29*, 427 – 432.
[12] a) J. Liu, C. Zhang, Z. Shen, W. Hua, Y. Tang, W. Shen, Y. Yue, H. Xu, *Catal. Commun.* **2009**, *10*, 1506 – 1509; b) H. E. van der Bij, B. M. Weckhuysen, *Chem. Soc. Rev.* **2015**, *44*, 7406 – 7428; c) J. C. Vedrine, A. Auroux, P. Dejaifve, V. Ducarme, H. Hoser, S. Zhou, *J. Catal.* **1982**, *73*, 147 – 160.
[13] M. Stöcker, *Microporous Mesoporous Mater.* **1999**, *29*, 3 – 48.
[14] L. Rodríguez-González, U. Simon, *Meas. Sci. Technol.* **2010**, *21*, 027003.
[15] S. Sartipi, K. Parashar, M. J. Valero-Romero, V. P. Santos, B. van der Linden, M. Makkee, F. Kapteijn, J. Gascon, *J. Catal.* **2013**, *305*, 179 – 190.
[16] J. Brus, L. Kobera, W. Schoefberger, M. Urbanova, P. Klein, P. Sazama, E. Tabor, S. Sklenak, A. V. Fishchuk, J. Dedecek, *Angew. Chem. Int. Ed.* **2015**, *54*, 541 – 545; *Angew. Chem.* **2015**, *127*, 551 – 555.
[17] a) Q. Zhao, W. H. Chen, S. J. Huang, Y. C. Wu, H. K. Lee, S. B. Liu, *J. Phys. Chem. B* **2002**, *106*, 4462 – 4469; b) A. Zheng, S.-J. Huang, W.-H. Chen, P.-H. Wu, H. Zhang, H.-K. Lee, L.-C. de Menorval, F. Deng, S.-B. Liu, *J. Phys. Chem. A* **2008**, *112*, 7349 – 7356.
[18] S. Hayashi, K. Jimura, N. Kojima, *Microporous Mesoporous Mater.* **2014**, *186*, 101 – 105.
[19] W.-H. Chen, H.-H. Ko, A. Sakthivel, S.-J. Huang, S.-H. Liu, A.-Y. Lo, T.-C. Tsai, S.-B. Liu, *Catal. Today* **2006**, *116*, 111 – 120.
[20] N.-L. Michels, S. Mitchell, J. Perez-Ramirez, *ACS Catal.* **2014**, *4*, 2409 – 2417.
[21] a) J. F. Haw, W. G. Song, D. M. Marcus, J. B. Nicholas, *Acc. Chem. Res.* **2003**, *36*, 317 – 326; b) R. Khare, D. Millar, A. Bhan, *J. Catal.* **2015**, *321*, 23 – 31.
[22] L. R. Aramburo, E. de Smit, B. Arstad, M. M. van Schooneveld, L. Sommer, A. Juhin, T. Yokosawa, H. W. Zandbergen, U. Olsbye, F. M. F. de Groot, B. M. Weckhuysen, *Angew. Chem. Int. Ed.* **2012**, *51*, 3616 – 3619; *Angew. Chem.* **2012**, *124*, 3676 – 3679.
[23] S. M. Abubakar, D. M. Marcus, J. C. Lee, J. O. Ehresmann, C. Y. Chen, P. W. Kletnieks, D. R. Guenther, M. J. Hayman, M. Pavlova, J. B. Nicholas, J. F. Haw, *Langmuir* **2006**, *22*, 4846 – 4852.
[24] a) M. Khanmohammadi, S. Amani, A. B. Garmarudi, A. Niaei, *Chin. J. Catal.* **2016**, *37*, 325 – 339; b) F. L. Bleken, S. Chavan, U. Olsbye, M. Boltz, F. Ocampo, B. Louis, *Appl. Catal. A* **2012**, *447*, 178 – 185.
[25] a) K. Omata, Y. Yamazaki, Y. Watanabe, K. Kodama, M. Yamada, *Ind. Eng. Chem. Res.* **2009**, *48*, 6256 – 6261; b) J. Li, S. Liu, H. Zhang, E. Lu, P. Ren, J. Ren, *Chin. J. Catal.* **2016**, *37*, 308 – 315.
[26] a) C. Mei, P. Wen, Z. Liu, H. Liu, Y. Wang, W. Yang, Z. Xie, W. Hua, Z. Gao, *J. Catal.* **2008**, *258*, 243 – 249; b) F. L. Bleken, K. Barbera, F. Bonino, U. Olsbye, K. P. Lillerud, S. Bordiga, P. Beato, T. V. W. Janssens, S. Svelle, *J. Catal.* **2013**, *307*, 62 – 73; c) J. Ahmadpour, M. Taghizadeh, *J. Nat. Gas Sci. Eng.* **2015**, *23*, 184 – 194.
[27] U. Olsbye, S. Svelle, K. P. Lillerud, Z. H. Wei, Y. Y. Chen, J. F. Li, J. G. Wang, W. B. Fan, *Chem. Soc. Rev.* **2015**, *44*, 7155 – 7176.
[28] a) C. D. Chang, C. T. W. Chu, R. F. Socha, *J. Catal.* **1984**, *86*, 289 – 296; b) C. T. W. Chu, C. D. Chang, *J. Catal.* **1984**, *86*, 297 – 300.
[29] J. Hafner, *J. Comput. Chem.* **2008**, *29*, 2044 – 2078.
[30] a) V. Van Speybroeck, K. De Wispelaere, J. Van der Mynsbrugge, M. Vandichel, K. Hemelsoet, M. Waroquier, *Chem. Soc. Rev.* **2014**, *43*, 7326 – 7357; b) V. Van Speybroeck, K. Hemelsoet, L. Joos, M. Waroquier, R. G. Bell, C. R. A. Catlow, *Chem. Soc. Rev.* **2015**, *44*, 7044 – 7111.
[31] a) A. V. Larin, G. M. Zhidomirov, D. N. Trubnikov, D. P. Vercauteren, *J. Comput. Chem.* **2010**, *31*, 421 – 430; b) G. Li, E. A. Pidko, R. A. van Santen, Z. Feng, C. Li, E. J. M. Hensen, *J. Catal.* **2011**, *284*, 194 – 206; c) G. Li, E. A. Pidko, R. A. van Santen, C. Li, E. J. M. Hensen, *J. Phys. Chem. C* **2013**, *117*, 413 – 426; d) G. Yang, Y. Wang, D. H. Zhou, X. C. Liu, X. W. Han, X. H. Bao, *J. Mol. Catal. A* **2005**, *237*, 36 – 44; e) G. M. Zhidomirov, A. V. Larin, D. N. Trubnikov, D. P. Vercauteren, *J. Phys. Chem. C* **2009**, *113*, 8258 – 8265.
[32] a) T. Armaroli, L. J. Simon, M. Digne, T. Montanari, M. Bevilacqua, V. Valtchev, J. Patarin, G. Busca, *Appl. Catal. A* **2006**, *306*, 78 – 84; b) C. Carteret, *J. Phys. Chem. C* **2009**, *113*, 13300 – 13308.
[33] C. A. Emeis, *J. Catal.* **1993**, *141*, 347 – 354.
[34] P. V. Wiper, J. Amelse, L. Mafra, *J. Catal.* **2014**, *316*, 240 – 250.
[35] B. M. Fung, A. K. Khitrin, K. Ermolaev, *J. Magn. Reson.* **2000**, *142*, 97 – 101.

Received: May 30, 2016
Published online on July 28, 2016